

Supporting Information

Understanding AuPd Alloy Nanoparticle Structure under Vacuum Using DFT and Monte Carlo Methods

Conor Waldt, Rajeev Kumar, David Hibbitts*

Department of Chemical Engineering, University of Florida, Gainesville, FL 32608, USA

*corresponding author: hibbitts@che.ufl.edu

Table of Contents

S1. Computational Methods.....	S3
S1.1 Particle Statistics.....	S3
Table S1	S3
S1.2 Monte Carlo Simulations.....	S3
Figure S1	S3
Figure S2.....	S4
Scheme S1.....	S5
S2. Exchange Energies.....	S6
S2.1 Exchange into Pure Au	S6
Figure S3.....	S6
Figure S4.....	S6
S2.2 Exchange with Pd in First and Second Coordination Shells	S7
Figure S5.....	S7
Table S2	S8
S2.3 Effects of Pd in the Extended Nanoparticle.....	S8
Figure S6.....	S9
Figure S7	S10
Figure S8.....	S11
Figure S9	S11
Figure S10.....	S11
Figure S11	S12
S3. Exchange Energy Models	S13
S3.1 Model Summaries	S13
Figure S12.....	S13
Table S3	S13
Table S4	S14
Table S5	S15
Table S6	S15
Figure S13.....	S16

S1. Computational Methods

S1.1 Particle Statistics

Table S1. Summary of statistics for the 201-atom Au particle.

Max Radius (nm)	Min Radius (nm)	Avg Radius (nm)	Avg. Diam (nm)	Num. Surf. Atoms	Dispersion	Avg. CN
0.9	0.7	0.8	1.7	122	0.6	9.4

S1.2 Monte Carlo Simulations

MC simulations require an input of temperature (273–573 K), Au/Pd ratio (1–200), and the maximum number of swaps (typically 2×10^5) and the ratio of swap-attempts to swaps (typically 100); these settings are defined in the PMC_settings.py file using python syntax (in Fig. S2). To define the structure of the nanoparticle, two files are also provided by the user: sites and neighbors. The sites file is a list of sites (positions within the nanoparticle) with the distance to the center of the nanoparticle, the coordination number of the site, the second coordination number, and the site-name provided in a space-separated list, one line per site. The neighbors file lists the atom-numbers (indexed to begin at 1) of all neighbors of each site in the particle. Both files have N lines, where N is the number of metal atoms in the particle. Examples of the sites and PMC_settings.py files are given in Figures S1 and S2, respectively, for the 201 atom particles simulated in this work.

In addition to these settings and structure-defining files, we also need to estimate the exchange energy for any atom within the particle as there are too many possible combinations to reasonably calculate all of them using DFT. Therefore, we estimate exchange energies (and thus swap energies) using a physical model (the CS-comp model specifically), as described below:

$$E_{Ex,est} = E_{Ex,0} + N_{CS1}E_{CS1} + N_{CS2}E_{CS2} \quad (\text{S1})$$

where $E_{ex,0}$ (kJ mol⁻¹) is the exchange energy for Pd into a dilute (1 Pd atom) Au nanoparticle at that specific exchange site, N_{CSX} and E_{CSX} (kJ mol⁻¹) are the number and the energy-penalty, respectively, of Pd atoms in the first (X=1) or second (X=2) coordination shell around the exchange site. Values for $E_{ex,0}$ are specified for each site-type in an input file: exch_nrg_1 (example in Fig. S1), and E_{CSX} is specified in PMC_settings.py (example in Fig. S2).

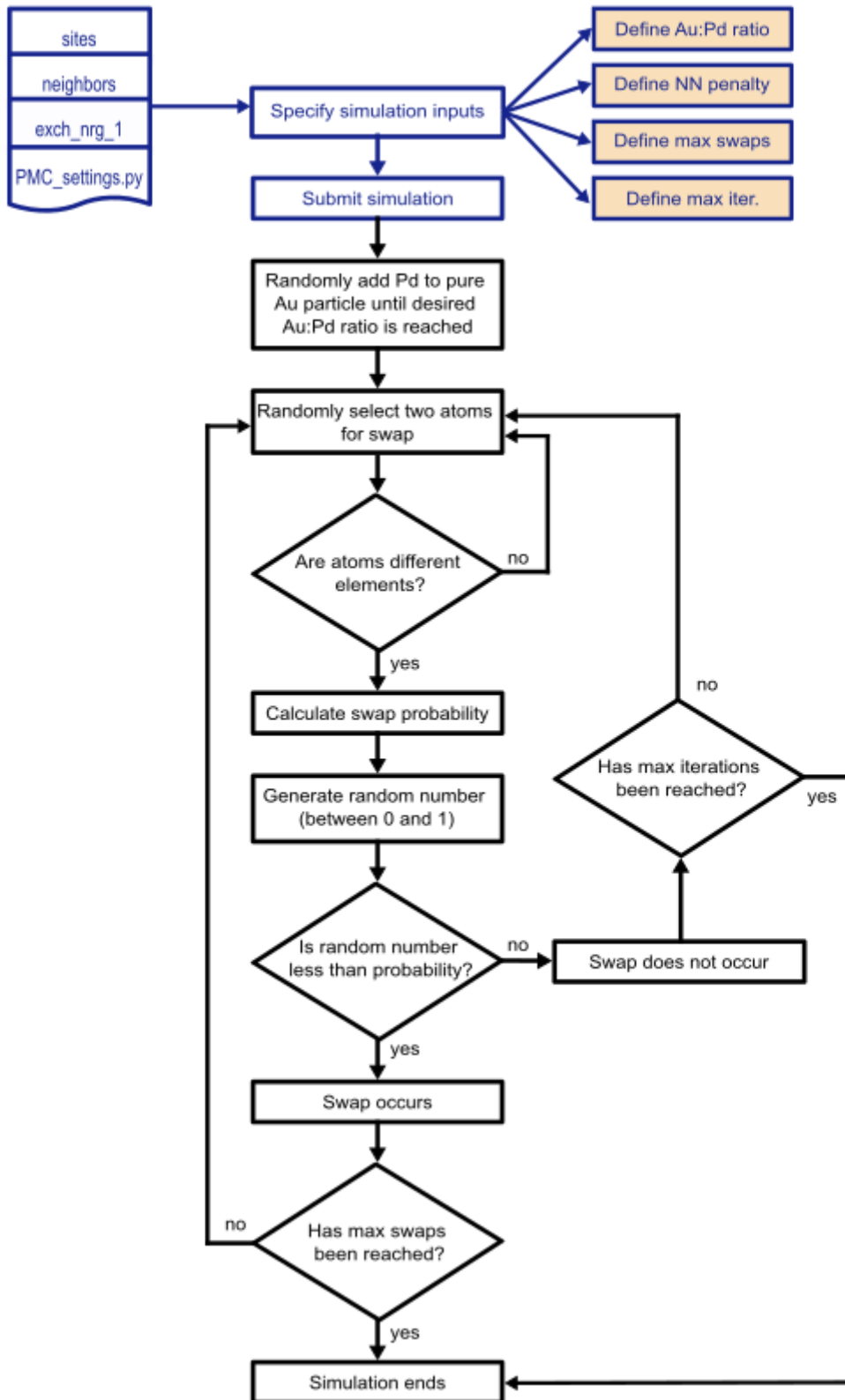
t111b	-14.2	7.05
t111a	-15.2	7.08
t100	-9.9	6.41
edge11	-1.3	7.92
edge10	-6.6	9.81
corner	1.4	9.45
sub1a	-51.4	7.35
sub1b	-43.4	5.86
sub1c	-50.1	7.85
sub2a	-56.5	9.24
sub2b	-49.8	8.03

sub3a -40.4 3.78

Figure S1. Example of the nrg_exch_1 file where the first column is the site type, the second column the exchange energy for putting a Pd at that site in a pure Au particle, and the last column is the is the penalty of Pd in the first coordination shell around that site. The third column is not currently used by the code, rather a regressed parameter is used.

```
Ma='Au'  
Mb='Pd'  
Mb_goal=50  
Temp=298  
nn_nrg=5.3  
iter_per_swap=100  
max_swaps=20  
pre_ads_swaps=5000  
iter_per_ads=100  
max_ads_des=50  
nnn_nrg=[-0.1801900, 0.07453211, 0.6133269]  
D5_nrg=-0.1137617  
P={}  
ads_list=[]
```

Figure S2. Example of the PMC_settings.py file. The nnn_nrg and D5_nrg values are not currently used by the code. P and ads_list are set up for future work dealing adsorbate systems.



Scheme S1. Workflow of the Monte Carlo simulations.

S2. Exchange Energies

S2.1 Exchange into Pure Au

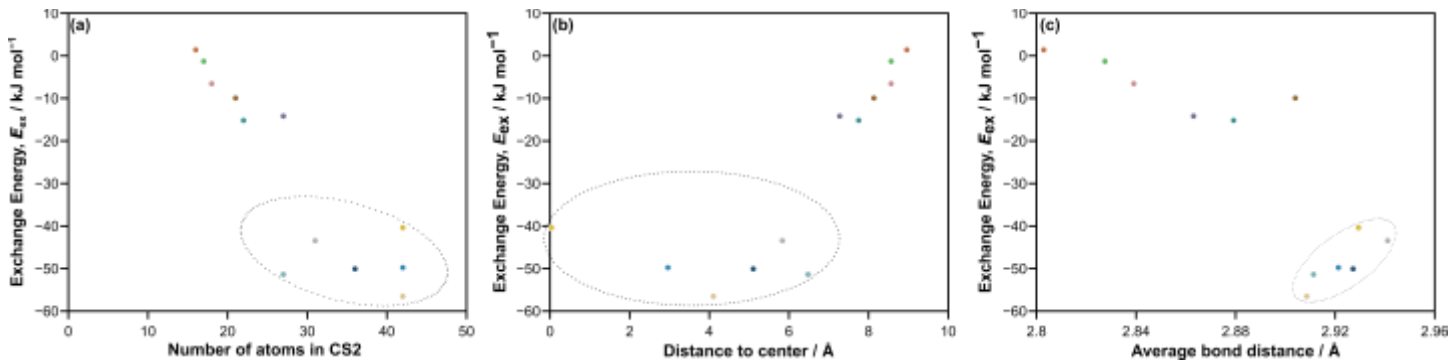


Figure S3. Exchange energies versus (a) number of neighbors of the atoms in CS2, (b) distance to the center of the particle from the exchange site, and (c) average bond distance around the exchange atom. Subsurface sites are circled in grey.

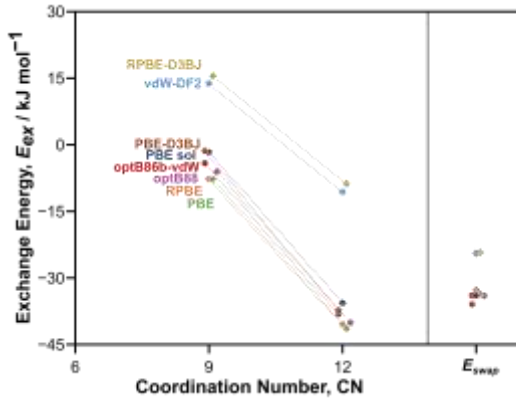


Figure S4. Exchange energies versus coordination number of the exchange site on a Au(111) slab model using different DFT functionals: RPBE (orange), RPBE-D3BJ (yellow), vdW-DF2 (light blue), PBE-D3BJ (brown), PBE sol (dark blue), optB86b-vdW (red), and PBE (green).

S2.2 Exchange with Pd in First and Second Coordination Shells

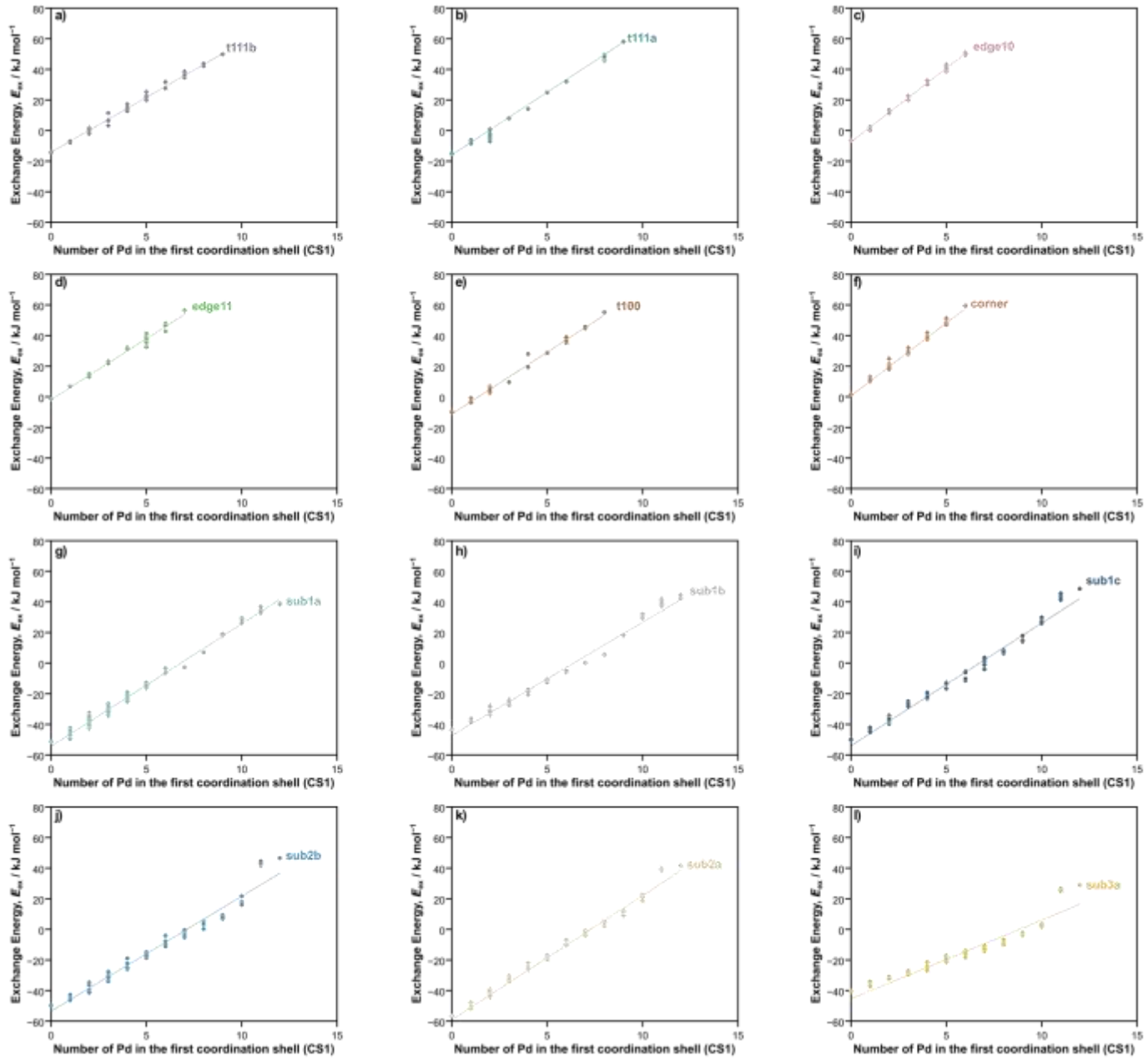


Figure S5. Exchange energies versus the number of Pd in the first coordination shell for each unique exchange site in the 201-atom particle model: (a) t111b (purple), (b) t111a (blue-green), (c) edge10 (pink), (d) edge11 (green), (e) t100 (brown), (f) corner (orange), (g) sub1a (sky blue), (h) sub1b (gray), (i) sub1c (dark blue), (j) sub2a (beige), (k) sub2b (light blue), and (l) sub3a (gold).

Table S2. Summary of the slopes of exchange energy versus number of Pd in the first and second coordination shells.

CS	corner	edge11	edge10	t100	t111a	t111b	sub1a	sub1b	sub1c	sub2a	sub2b	sub3a
Number	24	12	24	6	48	8	24	12	24	6	12	1
CS1	9.5	8.0	9.7	8.1	8.2	7.2	8.0	7.5	8.0	8.1	7.6	5.3
CS2	1.8	1.9	2.1	1.2	2.5	2.2	1.6	1.3	1.4	1.3	1.2	1.1

S2.3 Effects of Pd in the Extended Nanoparticle

In both the CS1 and extended nanoparticle exchange energy calculations, there is a clear discontinuity in the trend of exchange energy versus the number of Pd when going from 10 to 11 Pd (before exchange) as shown in Figures S5, S6a, and S7. This “jump” directly corresponds to a larger shift in the band energies going from 11 to 12 electrons (Fig. S8). Pd has one less valence electron than Au, so as the particle is filled with Pd, the total number of electrons is decreasing, shifting the highest filled band energy. Therefore, when going from 11 to 12 Pd it is not surprising that we see a large shift in exchange energies. We also investigated charged calculations where electrons were removed from the particle to create cationic particles. The second derivative of the system energy with respect to charge showed a value of ~0.4 eV higher for a charge of 11 ($z = 11$) as the charge is varied from 0 to 30, which is the same as the change in the energy levels obtained from the Au₂₀₁ (neutral) calculation (Fig. S9). A similar pattern can be seen for another “jump” in band energies around the 32nd highest energy level (corresponding to ~63 electrons) across all figures. Another measure of these electronic properties is the Fermi levels and indeed, we do see the same non-linear pattern that was observed for the exchange energies (Fig. S10a). However, the Fermi energies will change with Pd composition and arrangement, so we calculated an average Fermi energy at each Pd composition 0–201 Pd, for inclusion into our exchange energy models.

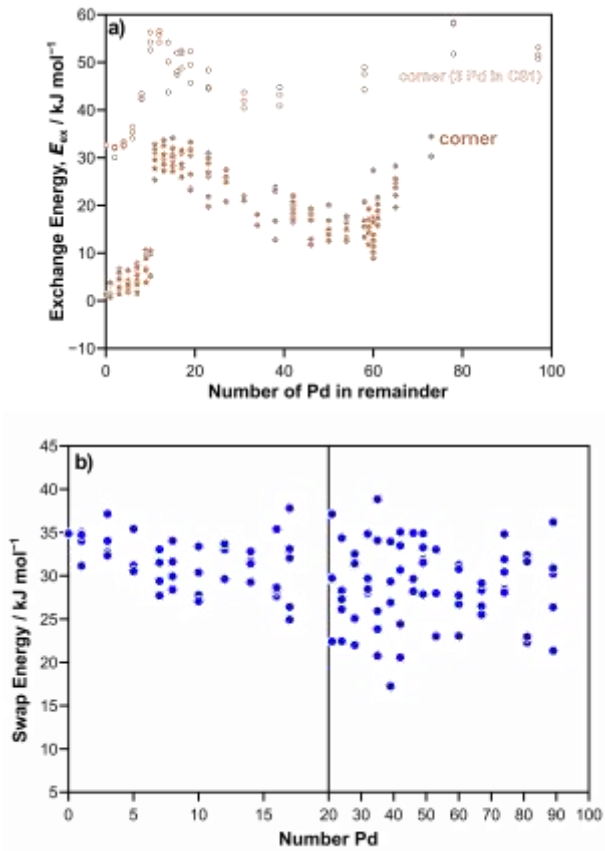


Figure S6. Plots for (a) exchange energies versus the number of Pd in the remainder of the particle for exchange at the corner site where 3 Pd are in CS1 (open circles) in comparison to the data with no Pd in CS1 (closed circles). Plot for (b) swap energy from the sub1c to t111b at changing Pd compositions in the remainder, for these data the first coordination shells of both sites were kept at pure Au (no Pd in either CS1).

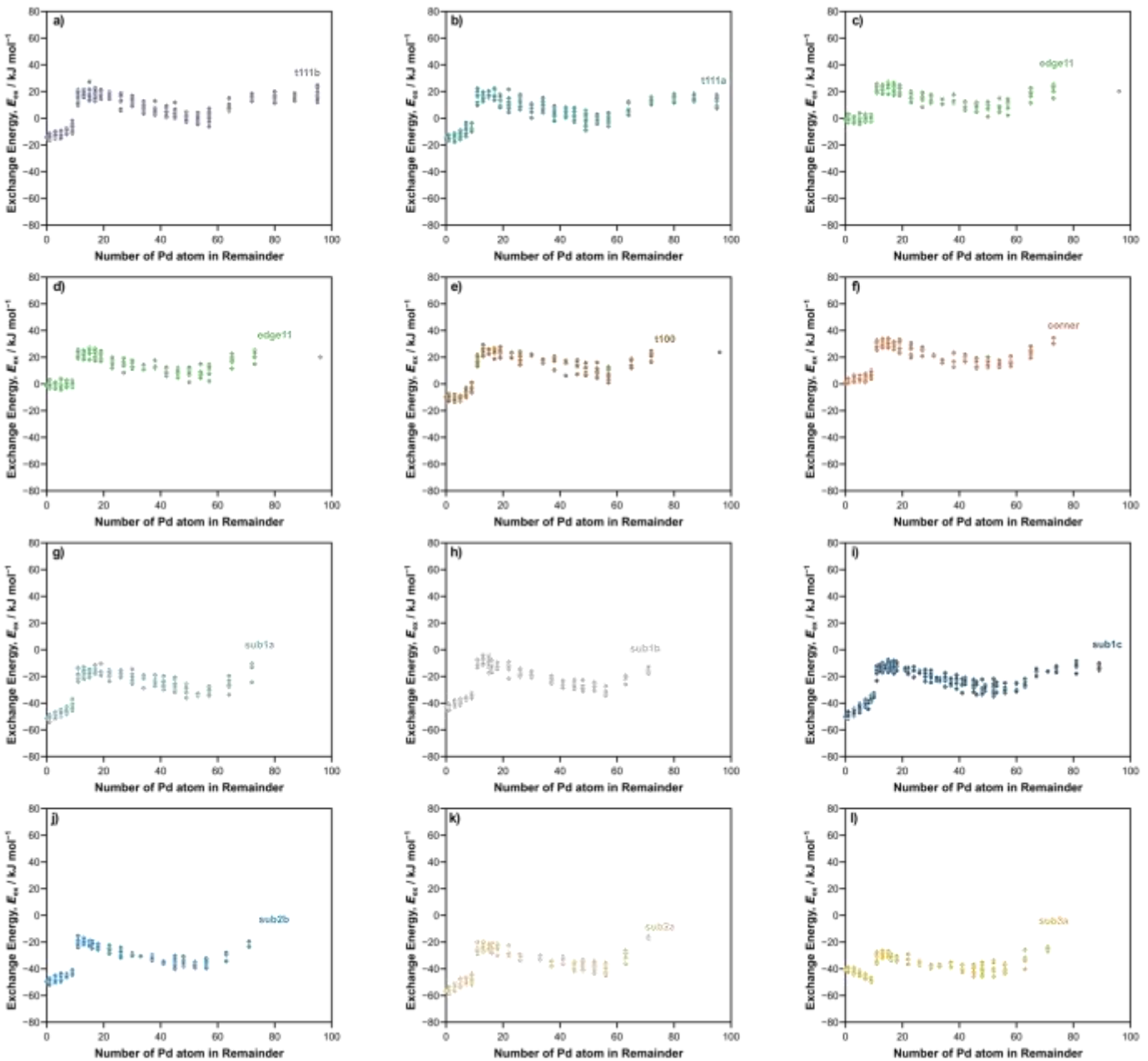


Figure S7. Exchange energies versus the number of Pd in the extended nanoparticle for each unique exchange site in the 201-atom particle model: (a) t111b (purple), (b) t111a (blue-green), (c) edge10 (pink), (d) edge11 (green), (e) t100 (brown), (f) corner (orange), (g) sub1a (sky blue), (h) sub1b (gray), (i) sub1c (dark blue), (j) sub2a (beige), (k) sub2b (light blue), and (l) sub3a (gold).

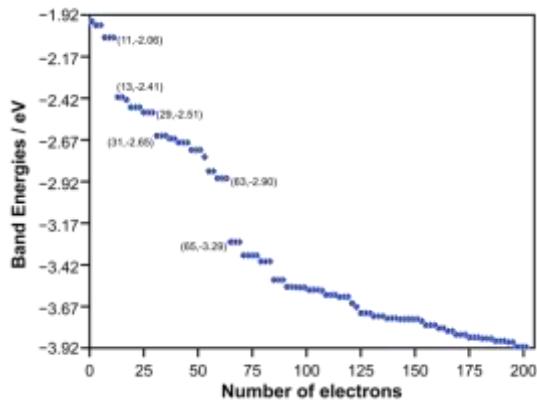


Figure S8. Band energies versus the number of valence electrons in a pure Au 201-atom particle.

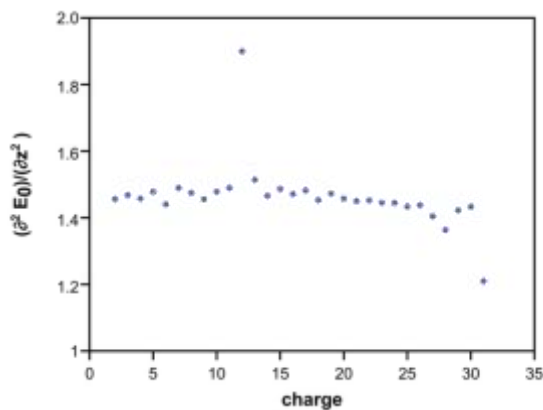


Figure S9. The second derivate of E_0 with respect to charge (e^-) plotted versus charge. These charged calculations were done by making a pure Au particle cationic through the removal of electrons and were performed with a uniform compensating background charge and dipole-corrected energies were used to calculate these values.

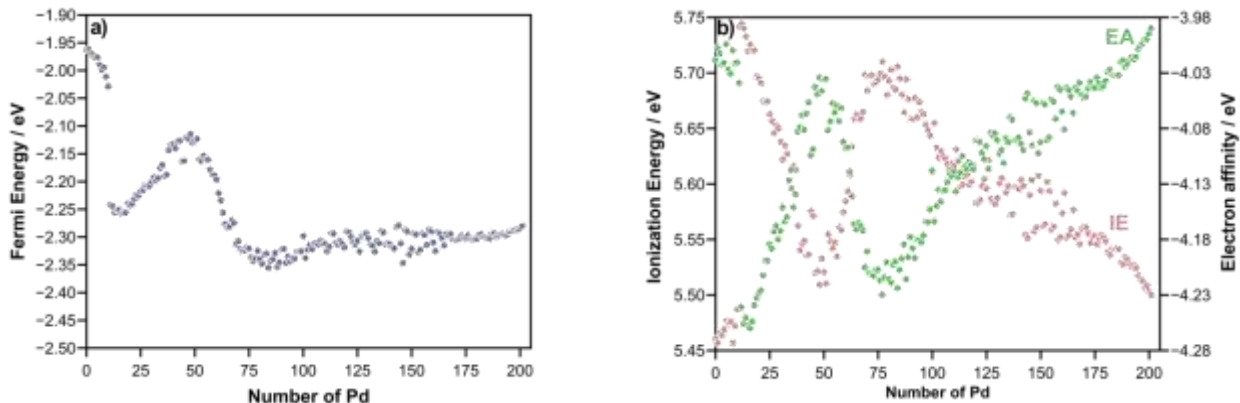


Figure S10. Plots of (a) the Fermi energy and (b) the ionization energy (pink) and electron affinity (green) versus the number of Pd in the extended nanoparticle.

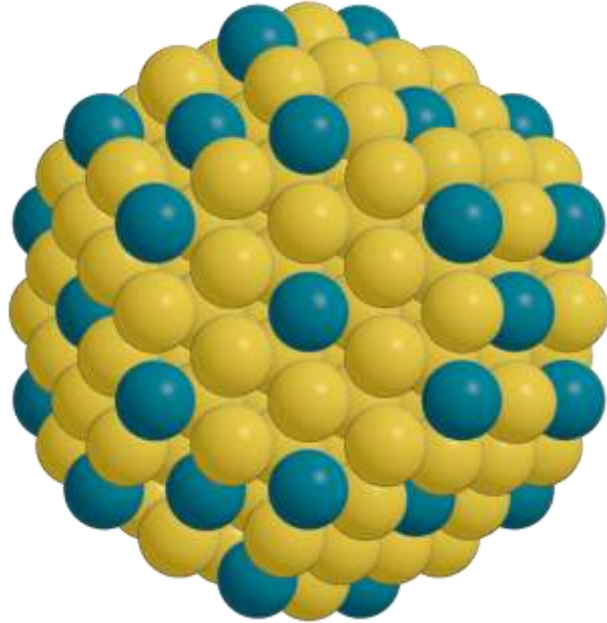


Figure S11. Structural image of the 201-atom particle with the theoretical maximum number (38) of monomeric Pd.

S3. Exchange Energy Models

S3.1 Model Summaries

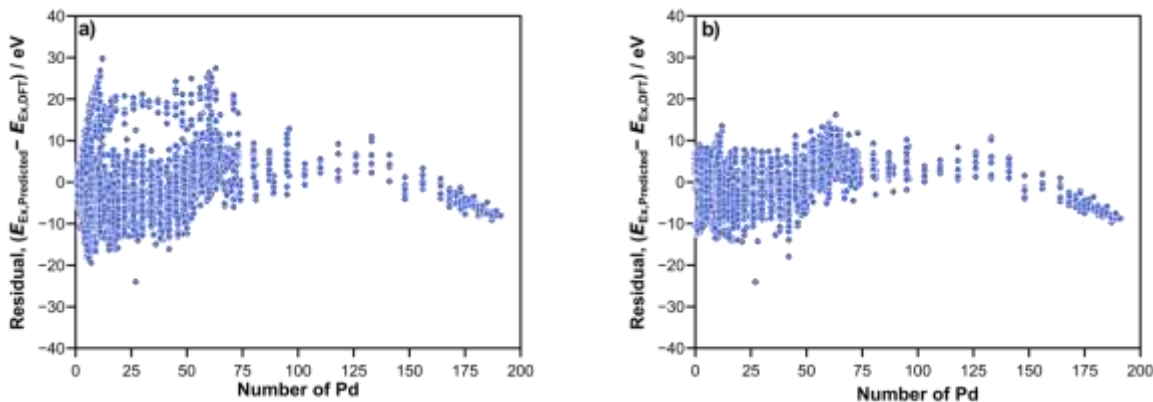


Figure S12. Residual plots for (a) the CS-based model and (b) the bond-energy model versus the number of Pd in the nanoparticle.

Table S3. Parameters for the CS-comp exchange energy model for both the 1 CS2 parameter (Eq. 5) and 3 CS2 parameter (Eq. 6) versions. Values in $\text{kJ mol}^{-1} \text{Pd}^{-1}$

Parameter	1 CS2 Param.	3 CS2 Param.
corner	1.39	1.39
edge10	-6.56	-6.56
edge11	-1.30	-1.30
sub1a	-51.37	-51.37
sub1b	-43.43	-43.43
sub1c	-50.06	-50.06
sub2a	-56.52	-56.52
sub2b	-49.76	-49.76
sub3a	-40.39	-40.39
t100	-9.94	-9.94
t111a	-15.19	-15.19
t111b	-14.17	-14.17
CS1	6.13	6.13
CS2	0.14	-0.30 0.22 0.20
Fermi (kJ mol ⁻¹)	-89.4	-89.6

Table S4. Parameters for bond energy model with 1 CS2 parameter (Eq. 9).

Au_sub_Pd_sub <-- Au_sub_Au_sub	-0.044	Pd_sub_Pd_sub <-- Au_sub_Pd_sub	0.016
Au_sub_Pd_t111 <-- Au_sub_Au_t111	0.002	Pd_sub_Pd_t111 <-- Pd_sub_Au_t111	0.052
Pd_sub_Au_t111 <-- Au_sub_Au_t111	-0.018	Pd_sub_Pd_t111 <-- Au_sub_Pd_t111	0.032
Au_sub_Pd_t100 <-- Au_sub_Au_t100	-0.012	Pd_sub_Pd_t100 <-- Pd_sub_Au_t100	0.051
Pd_sub_Au_t100 <-- Au_sub_Au_t100	-0.029	Pd_sub_Pd_t100 <-- Au_sub_Pd_t100	0.065
Au_sub_Pd_edge11 <-- Au_sub_Au_edge11	0.013	Pd_sub_Pd_edge11 <-- Pd_sub_Au_edge11	0.093
Pd_sub_Au_edge11 <-- Au_sub_Au_edge11	-0.039	Pd_sub_Pd_edge11 <-- Au_sub_Pd_edge11	0.020
Au_sub_Pd_edge10 <-- Au_sub_Au_edge10	0.000	Pd_sub_Pd_edge10 <-- Pd_sub_Au_edge10	0.082
Pd_sub_Au_edge10 <-- Au_sub_Au_edge10	-0.050	Pd_sub_Pd_edge10 <-- Au_sub_Pd_edge10	0.024
Au_sub_Pd_corner <-- Au_sub_Au_corner	0.000	Pd_sub_Pd_corner <-- Pd_sub_Au_corner	0.100
Pd_sub_Au_corner <-- Au_sub_Au_corner	-0.058	Pd_sub_Pd_corner <-- Au_sub_Pd_corner	0.012
Au_t111_Pd_t111 <-- Au_t111_Au_t111	-0.018	Pd_t111_Pd_t111 <-- Au_t111_Pd_t111	0.054
Au_t111_Pd_edge11 <-- Au_t111_Au_edge11	-0.016	Pd_t111_Pd_edge11 <-- Pd_t111_Au_edge11	0.061
Pd_t111_Au_edge11 <-- Au_t111_Au_edge11	0.001	Pd_t111_Pd_edge11 <-- Au_t111_Pd_edge11	0.027
Au_t111_Pd_edge10 <-- Au_t111_Au_edge10	0.003	Pd_t111_Pd_edge10 <-- Pd_t111_Au_edge10	0.090
Pd_t111_Au_edge10 <-- Au_t111_Au_edge10	-0.021	Pd_t111_Pd_edge10 <-- Au_t111_Pd_edge10	0.142
Au_t111_Pd_corner <-- Au_t111_Au_corner	0.046	Pd_t111_Pd_corner <-- Pd_t111_Au_corner	0.128
Pd_t111_Au_corner <-- Au_t111_Au_corner	-0.055	Pd_t111_Pd_corner <-- Au_t111_Pd_corner	0.030
Au_t100_Pd_edge10 <-- Au_t100_Au_edge10	-0.048	Pd_t100_Pd_edge10 <-- Pd_t100_Au_edge10	0.019
Pd_t100_Au_edge10 <-- Au_t100_Au_edge10	-0.004	Pd_t100_Pd_edge10 <-- Au_t100_Pd_edge10	0.075
Au_edge11_Pd_corner <--		Pd_edge11_Pd_corner <--	
Au_edge11_Au_corner	-0.084	Pd_edge11_Au_corner	0.005
Pd_edge11_Au_corner <--		Pd_edge11_Pd_corner <--	
Au_edge11_Au_corner	0.010	Au_edge11_Pd_corner	0.108
Au_edge10_Pd_corner <--		Pd_edge10_Pd_corner <--	
Au_edge10_Au_corner	0.014	Pd_edge10_Au_corner	0.109
Pd_edge10_Au_corner <--		Pd_edge10_Pd_corner <--	
Au_edge10_Au_corner	0.016	Au_edge10_Pd_corner	0.106
CS2	0.001		
E_fermi before	-0.853		

Table S5. Parameters for bond energy model with 3 CS2 parameter (Eq. 10).

Au_sub_Pd_sub <-- Au_sub_Au_sub	-0.044	Pd_sub_Pd_sub <-- Au_sub_Pd_sub	0.016
Au_sub_Pd_t111 <-- Au_sub_Au_t111	0.002	Pd_sub_Pd_t111 <-- Pd_sub_Au_t111	0.052
Pd_sub_Au_t111 <-- Au_sub_Au_t111	-0.017	Pd_sub_Pd_t111 <-- Au_sub_Pd_t111	0.032
Au_sub_Pd_t100 <-- Au_sub_Au_t100	0.011	Pd_sub_Pd_t100 <-- Pd_sub_Au_t100	0.073
Pd_sub_Au_t100 <-- Au_sub_Au_t100	-0.025	Pd_sub_Pd_t100 <-- Au_sub_Pd_t100	0.066
Au_sub_Pd_edge11 <-- Au_sub_Au_edge11	0.014	Pd_sub_Pd_edge11 <-- Pd_sub_Au_edge11	0.098
Pd_sub_Au_edge11 <-- Au_sub_Au_edge11	-0.041	Pd_sub_Pd_edge11 <-- Au_sub_Pd_edge11	0.004
Au_sub_Pd_edge10 <-- Au_sub_Au_edge10	-0.013	Pd_sub_Pd_edge10 <-- Pd_sub_Au_edge10	0.066
Pd_sub_Au_edge10 <-- Au_sub_Au_edge10	-0.052	Pd_sub_Pd_edge10 <-- Au_sub_Pd_edge10	0.022
Au_sub_Pd_corner <-- Au_sub_Au_corner	0.000	Pd_sub_Pd_corner <-- Pd_sub_Au_corner	0.098
Pd_sub_Au_corner <-- Au_sub_Au_corner	-0.058	Pd_sub_Pd_corner <-- Au_sub_Pd_corner	0.009
Au_t111_Pd_t111 <-- Au_t111_Au_t111	-0.018	Pd_t111_Pd_t111 <-- Au_t111_Pd_t111	0.053
Au_t111_Pd_edge11 <-- Au_t111_Au_edge11	-0.030	Pd_t111_Pd_edge11 <-- Pd_t111_Au_edge11	0.042
Pd_t111_Au_edge11 <-- Au_t111_Au_edge11	0.001	Pd_t111_Pd_edge11 <-- Au_t111_Pd_edge11	0.086
Au_t111_Pd_edge10 <-- Au_t111_Au_edge10	0.022	Pd_t111_Pd_edge10 <-- Pd_t111_Au_edge10	0.107
Pd_t111_Au_edge10 <-- Au_t111_Au_edge10	-0.015	Pd_t111_Pd_edge10 <-- Au_t111_Pd_edge10	0.107
Au_t111_Pd_corner <-- Au_t111_Au_corner	0.046	Pd_t111_Pd_corner <-- Pd_t111_Au_corner	0.131
Pd_t111_Au_corner <-- Au_t111_Au_corner	-0.059	Pd_t111_Pd_corner <-- Au_t111_Pd_corner	0.022
Au_t100_Pd_edge10 <-- Au_t100_Au_edge10	-0.059	Pd_t100_Pd_edge10 <-- Pd_t100_Au_edge10	0.021
Pd_t100_Au_edge10 <-- Au_t100_Au_edge10	-0.027	Pd_t100_Pd_edge10 <-- Au_t100_Pd_edge10	0.053
Au_edge11_Pd_corner <--		Pd_edge11_Pd_corner <--	
Au_edge11_Au_corner	-0.083	Pd_edge11_Au_corner	0.005
Pd_edge11_Au_corner <--		Pd_edge11_Pd_corner <--	
Au_edge11_Au_corner	0.038	Au_edge11_Pd_corner	0.142
Au_edge10_Pd_corner <--		Pd_edge10_Pd_corner <--	
Au_edge10_Au_corner	0.013	Pd_edge10_Au_corner	0.109
Pd_edge10_Au_corner <--		Pd_edge10_Pd_corner <--	
Au_edge10_Au_corner	0.015	Au_edge10_Pd_corner	0.105
CS2	-0.007		
	0.001		
	0.005		
E_fermi before	-0.853		

Table S6. Errors (in kJ mol⁻¹) for both models for 1 and 3 CS2 parameters.

Model	Num. CS2 Params.	SSE	RMSE	MAE
CS-Comp	1	2164	7.1	3.9
CS-Comp	3	2162	7.1	3.9
Bond-energy	1	1075	5.0	3.4
Bond-energy	3	1059	4.9	3.4

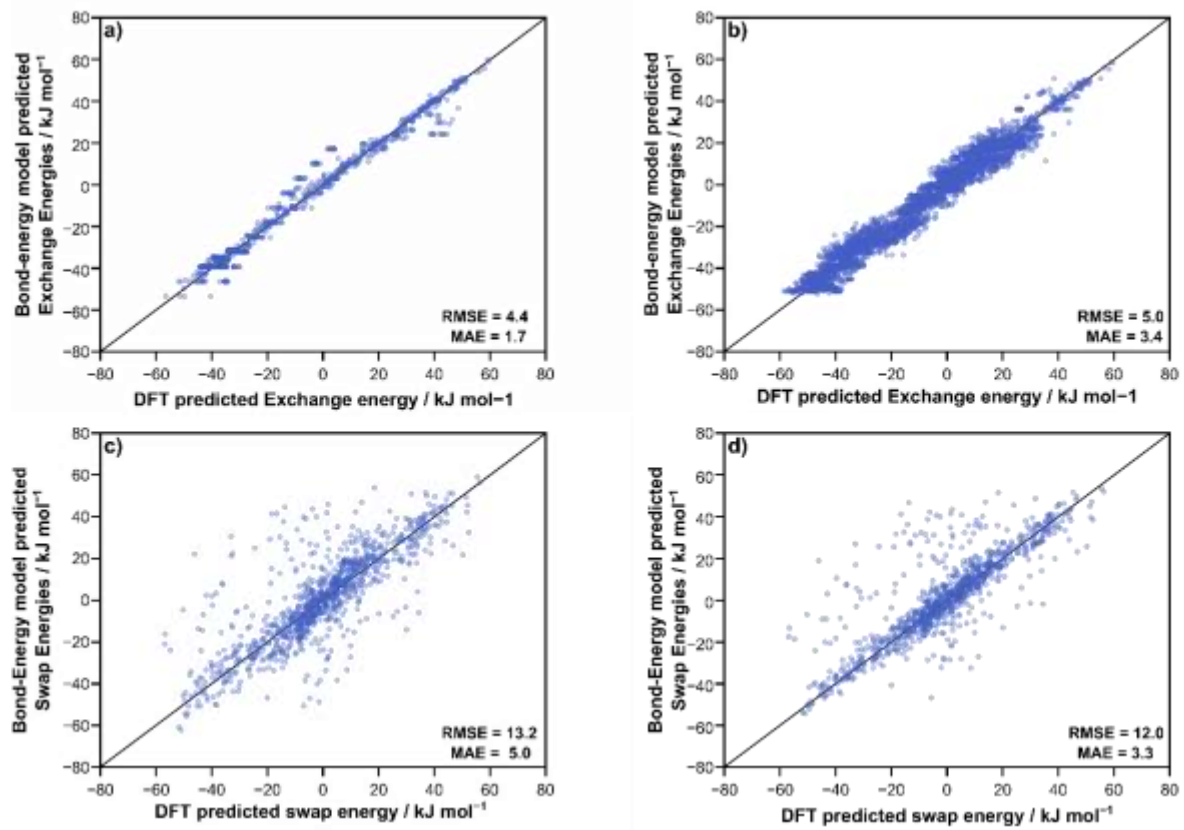


Figure S13. Parity plots for the (a-b) predicted exchange energies from the bond-energy model versus the DFT predicted energies and (c-d) predicted swap energies for using the bond energy exchange energies versus the DFT calculated energies using (a,c) a version of the model fit only with CS0 and CS1 data and (b,d) the full bond-energy model.